

1 MAPPING THE EPISTATIC NETWORK UNDERLYING MURINE

2 REPRODUCTIVE FATPAD VARIATION

3

4 Joseph P. Jarvis<sup>1,2</sup> and James M. Cheverud<sup>1</sup>

5

6 <sup>1</sup> Department of Anatomy & Neurobiology, Washington University School of Medicine,

7 St. Louis, Missouri, 63110

8 <sup>2</sup> Department of Genetics, University of Pennsylvania, Philadelphia, Pennsylvania, 19104

9

10

11

12

13

14

15

16

17

18

19

20

21

22

23

24 Running Title: Murine Fatpad Epistasis

25

26 Keywords: Genetic Architecture, Composite Interval Mapping, Pair-wise Interactions,

27 Epistatic Positional Candidates

28

29

30

31

32

33

34

35

36

37 Address Correspondence to:

38

39 Joseph P. Jarvis Ph.D.

40 Tishkoff Lab - Dept of Genetics

41 University of Pennsylvania

42 422 Clinical Research Building

43 415 Curie Blvd

44 Philadelphia, PA 19104-6145

45 215-746-2322

46 E-mail: [jarvisj@mail.med.upenn.edu](mailto:jarvisj@mail.med.upenn.edu)

47 ABSTRACT

48 Genome-wide mapping analyses are now commonplace in many species and  
49 several networks of interacting loci have been reported. However, relatively few details  
50 regarding epistatic interactions and their contribution to complex trait variation in multi-  
51 cellular organisms are available and the identification of positional candidate loci for  
52 epistatic QTL (epiQTL) is hampered, especially in mammals, by the limited genetic  
53 resolution inherent in most study designs. Here we further investigate the genetic  
54 architecture of reproductive fatpad weight in mice using the F<sub>10</sub> generation of the LG,SM  
55 Advanced Intercross (AI) line. We apply multiple mapping techniques including a  
56 single-locus model, locus-specific composite interval mapping, and tests for multiple  
57 QTL per chromosome to the twelve chromosomes known to harbor single locus QTL  
58 (sIQTL) affecting obesity in this cross. We also perform a genome-wide scan for pair-  
59 wise epistasis. Using this combination of approaches we detect 199 peaks spread over all  
60 19 autosomes that potentially contribute to trait variation including all eight original F<sub>2</sub>  
61 loci (*Adip1-8*), novel sIQTL peaks on chromosomes 7 and 9, and several novel epistatic  
62 loci. Extensive epistasis is confirmed involving both sIQTL confidence intervals as well  
63 as regions that show no significant additive or dominance effects. These results provide  
64 important new insights into mapping complex genetic architectures and the role of  
65 epistasis in complex trait variation.

66

66

## INTRODUCTION

67           The development and elaboration of techniques such as interval mapping (Lander  
68 and Botstein 1989), composite interval mapping (Zeng 1994), and methods based on  
69 complex pedigree structures (Jannink et al. 2001) has produced an extensive repertoire  
70 for the statistical exploration of genotype-phenotype relationships, especially for single  
71 loci. Using these approaches genome-wide analyses have identified single-locus QTL  
72 (sIQTL) underlying variance in characters as varied as agronomic traits and pest  
73 resistance in corn (Papst et al. 2004), life span in fruit flies (Wilson et al. 2006), alkylator  
74 induced cancer susceptibility in mice (Fenske et al. 2006), murine skeletal morphology  
75 (Kenney-Hunt et al. 2008), and an ever expanding list of human diseases and disorders  
76 including Age-Related Macular Degeneration (*e.g.* Klein et al. 2005), Type 2 diabetes  
77 (*e.g.* Sladek et al. 2007; Zeggini et al. 2008), and Crohn's disease (*e.g.* Duerr et al. 2006).  
78 In addition, several studies have successfully employed epistatic QTL (epiQTL) mapping  
79 strategies to describe multi-locus networks (*e.g.* Cheverud et al. 2001; Stylianou et al.  
80 2006; Wentzell et al. 2007; Fawcett et al. 2008, Fawcett et al. 2010).

81           However, most mapping studies in model systems involve either F<sub>2</sub> intercross  
82 populations or Recombinant Inbred (RI) strain panels (see also Hanlon et al. 2006).  
83 These populations harbor limited recombination and so tend to identify relatively large  
84 confidence intervals, complicating the physiological investigation of statistical results.  
85 Furthermore, while recombinant Inbred (RI) strain sets represent a four-fold expansion of  
86 the F<sub>2</sub> recombination-based map, they require a minimum of 20 generations of brother-  
87 sister mating (Silver 1995) and the number of strains per set is usually low, especially in  
88 mammals. Conversely, the production of Advanced Intercross (AI) lines involves many

89 generations of outbreeding in a relatively large population. This preserves  
90 heterozygosity, retains many more recombinant gametes in the gene pool, decreases the  
91 average size of segregating linkage blocks, and increases mapping resolution (Haldane  
92 and Waddington 1931; Bartlett and Haldane 1935; Hanson 1959a; Hanson 1959b;  
93 Hanson 1959c; Hanson 1959d; Darvasi and Soller 1995; Rockman and Kruglyak 2008).  
94 Specifically, the F<sub>10</sub> generation of a murine AI line represents an approximately five-fold  
95 expansion of the F<sub>2</sub> map and thus an improvement in resolution over both F<sub>2</sub> intercross  
96 and RI line study designs.

97 Obesity and related phenotypes are among the most intensively studied complex  
98 traits in mice and the LG,SM AI has proven particularly useful in the identification of  
99 adiposity QTLs. Previous work in this cross has characterized over 70 loci contributing  
100 to variance in fatpad weight, body weight and relevant organ weights (Cheverud et al.  
101 1999; Cheverud et al. 2001; Cheverud et al. 2004; Fawcett et al. 2008). In addition, a  
102 recent study used the combined F<sub>9</sub> and F<sub>10</sub> generations (Fawcett et al. 2010) to fine-map  
103 loci for a suite of obesity related characters and achieved an average confidence interval  
104 for fatpad loci of 4.14 Mb. These CI were subsequently tested for epistasis and extensive  
105 interaction was confirmed, though several direct effect loci identified in the F<sub>2</sub> and F<sub>2/3</sub>  
106 generations failed to replicate and were thus not included. However, in a full genome-  
107 wide scan for pair-wise epistasis in the F<sub>2</sub> generation of this cross (Jarvis and Cheverud  
108 2009) 38 fatpad loci that were not identified using a single locus mapping model show  
109 significant epistatic interactions. Consistent with results from other experimental systems  
110 (reviewed in Phillips 2008) this suggests that many biologically relevant loci are invisible  
111 to single locus scans. Thus, combining the increased genetic resolution of an F<sub>10</sub> AI line

112 study, with the full range of single-locus and epistatic mapping strategies promises to  
113 produce novel insights into the contribution of epistatic interactions to variation in  
114 reproductive fatpad weight in mice. Furthermore, the accumulating data on positional  
115 candidate genes (*e.g.* Chehab 2008; Gat-Yablonski and Phillip 2008; Ichihara and  
116 Yamada 2008; Cheverud et al. 2009) provides the opportunity to explore functional  
117 hypotheses for identified loci and their interactions.

118 Utilizing the F<sub>10</sub> generation of the LG,SM AI line (Cheverud et al. 2001) we  
119 further characterized the complex genetic architecture underlying murine reproductive  
120 fatpad weight. We first performed a slQTL scan on the original eight chromosomes  
121 harboring direct effect loci in the F<sub>2</sub> generation (1, 6, 7, 8, 9, 12, 13, and 18) as well as  
122 the four shown to harbor slQTL in the combined F<sub>9</sub>-F<sub>10</sub> population (3, 4, 10 and 16;  
123 Fawcett et al. 2010). Composite interval mapping and two-QTL tests were subsequently  
124 performed, the latter when multiple loci on a single chromosome were suspected.  
125 Finally, we carried out a full genome-wide scan for pair-wise epistasis. In order to  
126 identify the most meaningful set of loci to screen for candidate genes, marker genotypes  
127 representing slQTL and epiQTL that exceeded their appropriate thresholds were  
128 combined in linear models, first for each chromosome separately and ultimately the entire  
129 genetic system. Confidence intervals for peaks that remained significant in the full model  
130 were screened for positional candidate loci and potential physiological interactions via  
131 both the MGI database ([www.informatics.jax.org/](http://www.informatics.jax.org/)) and a literature search.

132

133

## MATERIALS AND METHODS

134           **Data:** The population analyzed is the F<sub>10</sub> generation (N = 1298; 85 full-sib  
135 families; average litter size 8.45) of an Advanced Intercross (AI) line generated from an  
136 F<sub>2</sub> intercross of the inbred mouse strains SM/J and LG/J (Chai 1956; Chai 1956;  
137 Cheverud et al. 1996; Vaughn et al. 1999; Cheverud et al. 2001). The animal facility is  
138 maintained at a constant temperature of 21°C with 12-hour light-dark cycles. Animals  
139 were fed a standard rodent chow (PicoLab Rodent Chow 20 (#5053) with 12% of its  
140 energy from fat, 23% from protein, and 65% from carbohydrate) *ad libitum* and were  
141 weaned at 3 weeks of age. After weaning, animals were housed in single sex cages  
142 containing no more than 5 individuals.

143           Between the F<sub>2</sub> and F<sub>10</sub> generations the population was maintained at an effective  
144 size of approximately 300 with 75 mating pairs and no variance in family size. Mating  
145 between littermates was actively avoided. At greater than 13 weeks of age animals were  
146 sacrificed and necropsies performed. The reproductive fatpads of each animal were  
147 removed, combined and weighed on a digital scale to the nearest hundredth of a gram.  
148 Phenotypes were statistically corrected for age at necropsy, sex, litter size, and parity  
149 status (whether or not they were mated to produce the F<sub>11</sub>) using multiple regression and  
150 the residuals used for further analysis. Genotypes for each individual were obtained at  
151 1470 polymorphic SNPs across the genome by Illumina (San Diego, USA) GoldenGate  
152 Assay using DNA extracted from liver tissue obtained at necropsy. Inter-marker  
153 genotypes were imputed at 1 cM intervals using the equations of Haley and Knott (1992).

154           **Mapping Analyses:** A single locus QTL (slQTL) scan at all measured and  
155 imputed loci was first conducted on chromosomes 1, 3, 4, 6, 7, 8, 9, 10, 12, 13, 16, and  
156 18 using the regression model:

157

$$158 \quad Y_i = \mu + a * X_{ai} + d * X_{di} + \text{error} \quad (1)$$

159

160 where  $Y_i$  is the vector of corrected phenotypes,  $\mu$  is a constant, and  $X_{ai}$  and  $X_{di}$  are the  
161 vectors of genotype scores;  $a$  and  $d$  are the fitted additive and dominance regression  
162 coefficients respectively. The sums of squares for both model terms were pooled for  
163 significance testing. The results of the full genome-wide sIQTL mapping in the  
164 combined F<sub>9</sub>-F<sub>10</sub> generations were previously reported (Fawcett et al. 2010).

165 Composite interval (CI) mapping (Zeng 1994) was applied to the identified,  
166 preliminary confidence intervals using the following model:

167

$$168 \quad Y_{ijk} = \mu + a * X_{ai} + d * X_{di} + \text{error} \mid X_{aj} X_{dj} X_{ak} X_{dk} \quad (2)$$

169

170 In this case,  $X_{aj}$ ,  $X_{dj}$ ,  $X_{ak}$ , and  $X_{dk}$  represent vectors of genotype scores at loci greater than  
171 20 F<sub>10</sub> cM up- and down-stream of the confidence interval on whose effects the within-  
172 interval regressions were conditioned. This eliminates the effects of proximal and distal  
173 QTL on the same chromosome from being confounded with the target QTL. When  
174 multiple peaks on the same chromosome were suggested, the fit of all pair-wise two locus  
175 models were compared to the appropriate single locus case using a  $X^2$  test with two  
176 degrees of freedom ( $X^2_{\text{crit}} = 2 * \text{abs}[\ln(1/p_{\text{one}}) - \ln(1/p_{\text{two}})]$ ), where  $p_{\text{one}}$  and  $p_{\text{two}}$  are p-values  
177 from the one and two locus models respectively (Sokal and Rohlf 1995).



178 Finally all genome-wide, between-chromosome, pair-wise combinations of  
179 measured and imputed autosomal loci were tested using the following epistatic mapping  
180 model:

181

$$182 Y_{ij} = \mu + aa(X_{ai} * X_{aj}) + ad(X_{ai} * X_{dj}) + da(X_{di} * X_{aj}) + dd(X_{di} * X_{dj}) + \text{error} \mid X_{ai} X_{di} X_{aj} X_{dj} \quad (3)$$

183

184 where *aa*, *ad*, *da*, and *dd* are the additive-by-additive, additive-by-dominance,  
185 dominance-by-additive, and dominance-by-dominance epistasis regression coefficients  
186 and  $X_{ai} X_{di} X_{aj} X_{dj}$  represent vectors of the corresponding additive and dominance  
187 genotypes at the two loci involved. The sums of squares and degrees of freedom for all  
188 four epistatic components were pooled for initial significance testing. The raw  
189 probability associated with each multiple regression for all mapping analyses above was  
190 transformed to a linear scale using the base 10 logarithm of the inverse of the probability  
191 of no epistasis ( $LPR = \log_{10}(1/p)$ ) producing values comparable to LOD scores obtained  
192 through maximum likelihood analysis (Lander and Botstein 1989).

193 **Thresholds:** Interpretation of these analyses is complicated both by the large  
194 number of comparisons involved as well as the family structure present in the population.  
195 In order to account for these two issues simultaneously, simulations were performed  
196 using the known pedigree of all individuals between the  $F_2$  and  $F_{10}$  generations to  
197 generate a null distribution of expected effects from which the appropriate single-locus  
198 LPR threshold was determined (Fawcett et al. 2008, Norgard et al. 2009). Given a  
199 heritability of reproductive fatpad weight in the  $F_{10}$  of 0.47 (from sib-correlations)  
200 chromosome-specific thresholds for identifying novel sLQTL ranged from 6.15

201 (chromosome 8) to 6.6 (chromosome 1). The experiment-wide threshold for novel sQTL  
202 detection was 7.34. For the purposes of replication, a corrected point-wise threshold  
203 (equivalent to  $p = 0.05$ ) of 3.32 was applied for sQTL peaks within previously identified  
204 confidence intervals.

205       Following the method described in Fawcett et al. (2010), the analysis-wide  
206 epistasis threshold for the identification of novel interactions was calculated to be 8.33.  
207 The threshold for tests between a given sQTL and all other unlinked markers in the  
208 analysis was 6.06 and the analogous chromosome-specific thresholds ranged from 4.73  
209 (chromosome 8) to 5.25 (chromosome 1). The corrected point-wise threshold for  
210 epistatic tests between two sQTL was 3.44. Tests involving sQTL are partially  
211 protected from multiple comparisons as they were identified with independent  
212 information.

213       **Confidence Intervals:** Due to the complexity of our mapping strategy, the  
214 conventional 1 LPR drop criterion was applied to define all reported confidence intervals.  
215 When multiple peaks, either sQTL, epiQTL or both, occurred in the same region, the  
216 most proximal and most distal 1 LPR drop was used to determine CI endpoints.  
217 Confidence intervals (CI) for sQTL peaks were also calculated for each location  
218 individually using the standard deviation of the simulated distribution of 1000 mapping  
219 iterations involving known effects on simulated chromosomes (Norgard et al. 2009). The  
220 two techniques yielded very similar CI for all sQTL though the simulation-based  
221 intervals were slightly smaller.

222       **Linear Models:** We constructed and evaluated separate chromosome-specific  
223 models using the linear model function in R (R Development Core Team) before

224 combining their results into a full model of the genetic system. This process began with  
225 terms representing each significant effect at all slQTL peaks identified by the single locus  
226 model (equation 1) and composite interval mapping (equation 2). For example, the  
227 chromosome 1 model (see Figure 1A) began with five slQTL terms representing the  
228 additive ( $p = 0.00726$ ) and dominance ( $p = 0.0007$ ) effects at 20.15 Mb, the additive ( $p =$   
229  $0.000268$ ) and dominance ( $p = 0.0383$ ) effects at 70.77 Mb and the dominance effect ( $p =$   
230  $1.06 \times 10^{-06}$ ) at 134.82 Mb. The additive effect at 134.82 Mb was non-significant in the  
231 slQTL mapping model ( $p = 0.868$ ) and so was not included. Likewise, the chromosome  
232 13 model (see Figure 1B) included two terms representing the additive effects at 53.54  
233 Mb ( $p = 3.05 \times 10^{-06}$ ) and 90.61 Mb ( $p = 4.88 \times 10^{-05}$ ) respectively. In this case, neither  
234 dominance effect was significant in the slQTL mapping model ( $p = 0.798$  and  $p = 0.634$ )  
235 and so both were excluded. When considered jointly, some individual terms (*e.g.* the  
236 dominance effect only at 70.77 Mb on chromosome 1) no longer remained significant ( $p$   
237  $< 0.05$ ) in Type I ANOVA tables (using the “anova” function). Such terms were  
238 removed. For those chromosomes not found to harbor slQTL, a similar process was  
239 performed beginning with all significant interactions.

240       Next, individual coefficients from the epistatic mapping model ( $aa, ad, da, dd$ ;  
241 equation 3) at all peaks that exceeded their appropriate thresholds in the epiQTL scan  
242 were similarly examined to determine the type or types of interactions occurring. Terms  
243 representing all significant interactions were then added step-wise to each appropriate  
244 chromosome-specific model. Only epistatic terms that remained significant ( $p < 0.05$ ) in  
245 both Type I and Type II ANOVA tables, using the R functions “anova” and “Anova” (the  
246 latter from the package “car”) respectively and did not cause any established additive or

247 dominance effects to become non-significant ( $p < 0.05$ ) were retained to define each final  
248 chromosome-specific model. These stringent criteria were established in order to obtain  
249 a tractable number of high-confidence CI to screen for positional candidates and  
250 physiological interactions.

251         Next, additive and dominance terms from all chromosome-specific models were  
252 combined and terms that became non-significant in either Type I or Type II ANOVA  
253 tables (or both) were culled to define the “slQTL system.” This model included 20 terms  
254 at 18 loci (15 additive and 5 dominance; bold in Supplemental Table 1). Epistasis terms  
255 significant in the chromosome-specific models were then added stepwise to the slQTL  
256 system as above to define the “full model.” In addition to the 20 marginal effect terms,  
257 this model includes 23 interaction involving 26 different epiQTL confidence intervals.  
258 Finally, since many epiQTL peaks occur at locations not represented in the slQTL  
259 system, the appropriate additive and dominance terms for each interaction were added to  
260 the full model to ensure that the identified epistatic contributions were not unduly biased  
261 upward by variance attributable to single locus effects. This had relatively little effect  
262 and resulted in the elimination of only 3 interactions, all of which are significant in Type  
263 I tests. The results from the full model are reported with these nominally significant  
264 terms noted in bold (Table 1, see below).

265         **Candidate Genes:** All CI for peaks identified in the full model were screened for  
266 plausible positional candidate genes and known interactions. This involved both queries  
267 of the MGI database for functional variants affecting adiposity as well as a broad  
268 literature search and was intended to generate meaningful and testable physiological  
269 hypotheses regarding the observed statistical associations.

270

271

## RESULTS

272

273

274

275

276

277

278

279

280

281

282

283

284

285

286

287

288

289

290

291

292

**Replication and Identification:** Significant marginal effects, epistatic effects or both are observed in the F<sub>10</sub> population on all eight chromosomes harboring the original *Adip* loci and three of the four additional chromosomes implicated in the combined F<sub>9</sub>-F<sub>10</sub> sIQTl scan (Supplementary Figure 1). In the F<sub>10</sub> alone, there were no significant sIQTl on chromosome 16. Similar to the results of Fawcett et al. (2010), peak LPR scores from either the single locus scan or composite interval mapping at or near the confidence intervals of five *Adip* loci exceeded the experiment-wide threshold (7.34) even for novel QTL detection (*Adip1*: LPR = 9.2, *Adip2*: LPR = 8.9, *Adip3*: LPR = 8.3, *Adip5*: LPR = 9.6, and *Adip8*: LPR = 12.3). All three remaining F<sub>2</sub> loci exceed the point-wise threshold (3.32) required for tests within previously defined confidence intervals (*Adip4*: LPR = 5.6, *Adip6*: LPR = 5.24; *Adip7*: LPR = 4.8). Additional sIQTl on chromosomes 3, 4, and 10 also replicated. Interestingly, the chromosome 4 locus (*Adip24*, Fawcett et al. 2010; LPR = 12.65) roughly corresponds to two loci previously reported in the literature as *Adip11* and *Adip12* in a cross between C57BL/6J and DBA/2J (Keightley et al. 1996; Brockmann et al. 1998; Stylianou et al. 2006). Finally, composite interval mapping revealed novel loci on chromosomes 7 and 9 that both exceed their appropriate chromosome-specific thresholds of 6.36 and 6.38 respectively. A total of 22 potential marginal effect peaks were identified (Supplementary Table 1).

**epiQTL Mapping:** In the genome-wide scan for epistasis 177 peaks involving 217 interactions exceeded their appropriate significance thresholds and physically cluster into approximately 51 potential epiQTL (Supplementary Table 1). Additive-by-additive

293 interactions were the most common (98), Additive-by-Dominance or Dominance-by-  
294 Additive were the next most common (97) and Dominance-by-Dominance interactions  
295 were the most rare (22). Consistent with the results of Jarvis and Cheverud (2009) and  
296 several other studies (see Phillips 2008), many of these occurred at locations showing no  
297 significant marginal effects in this cross, though some occurred at locations significant in  
298 slQTL scans in other crosses (Table 1; Figure 1; Supplementary Table 1; Supplementary  
299 Figures 2-20).

300       **Linear Models:** In total, we identified 199 slQTL and epiQTL peaks that  
301 potentially contribute to trait variation. These cluster into roughly 73 confidence  
302 intervals showing a variety of combinations of additive, dominance and epistatic effects  
303 (Supplementary Table 1). In order to identify the most robust signals we systematically  
304 added vectors of genotype scores representing each into linear models and determined the  
305 set that is simultaneously significant in both Type I and Type II tests. We began by  
306 establishing a single locus model that contained all slQTL peaks that remain significant  
307 together. This slQTL system includes 20 marginal effect terms (15 additive and 5  
308 dominance) shows an adjusted  $R^2$  value of 0.2254 (F statistic = 18.64 on 20 and 1281 df).  
309 We next added epistatic peaks stepwise to generate a full model of the genetic system.  
310 This full model (Table 1) includes 23 additional interaction terms (9 *aa*, 10 *ad/da*, and 4  
311 *dd*) involving 26 different epiQTL confidence intervals and shows an adjusted  $R^2$  value  
312 of 0.3322 (F statistic = 15.71 on 43 and 1257 df). Using a chi-square goodness of fit test  
313 with 23 (43-20) degrees of freedom this represents a highly significant improvement in fit  
314 over the base slQTL model ( $p < 10^{-25}$ ). Following the addition of all marginal terms  
315 involved in epistasis, three interaction terms become non-significant at the  $p < 0.05$  level

316 in either the Type I or the Type II tables or both (bold terms in Table 1). Removing these  
317 interactions from the full model, its adjusted  $R^2$  value is 0.3220 (F statistic = 16.07 on 40  
318 and 1260 df), which also represents a highly significant improvement in model fit ( $p <$   
319  $10^{-20}$ ).

320         **Positional Candidates:** While in-depth functional assays and other detailed  
321 molecular studies are required to sort out the biological basis of QTL and their  
322 interactions, examination of positional candidate genes in sIQTL confidence intervals  
323 suggests testable physiological hypotheses for several observed statistical effects. In  
324 general, confidence intervals contain a variety of candidate loci including transcription  
325 factors, components of various signaling cascades (*e.g.* the *Wnt*, *Insulin*, and *Igf* signaling  
326 networks), neuro-endocrine hormones and their receptors, as well as genes directly  
327 implicated in glucose processing and metabolism. For example, the CI found at  
328 6:133.92-142.67 Mb contains the promising candidate *Lrp6*, a low-density lipoprotein  
329 receptor-related protein that is thought to contribute to variation in a variety of metabolic  
330 risk factors in humans (Kahn et al. 2007; Mani et al. 2007) and *Cdkn1b*, a cyclin-  
331 dependent kinase inhibitor with known effects on pancreatic islet mass in diabetic mice  
332 (Uchida et al. 2005). Both *Lrp6* and *Cdkn1b* have differences in expression level in  
333 white fat ( $p = 3.82 \times 10^{-12}$  and 0.013, respectively) and in the liver ( $p = 1.62 \times 10^{-13}$  and  
334  $7.48 \times 10^{-8}$ , respectively) between the two parental lines in this cross (Cheverud,  
335 unpublished results). The CI 18:58.77-80.76 Mb shows potential functional links to  
336 mammalian neurotransmitter signaling via *Htr4* (Gardner et. al. 2008), as do 13:40.74-  
337 55.35 Mb via *Cplx2* (Brachya et al. 2006) and *Drd1a* (de Leeuw van Weenen et al. 2009).  
338 In addition, the region 6:114.73-121.97 Mb contains neuro-endocrine candidates *Adipor2*

339 (Yamauchi et al. 2007; Ziemke and Mantzoros 2010) and *Ankrd26* (Bera et al. 2008),  
340 which also shows a significant difference in expression in liver between LG/J and SM/J  
341 ( $p = 0.0002$ ; Cheverud, unpublished results). Together, these loci suggest a functionally  
342 similar genetic architecture to the emerging picture of Type 2 diabetes in humans (Doria  
343 et al. 2008).

344         There are also a number of strong candidate loci for observed epistatic  
345 interactions. The most striking involves the CIs 13:0-24.24 Mb and 1:118.37-138.01 Mb,  
346 which contain *Inhba* and *Inhbb* respectively. The proteins encoded by these loci are  
347 components of the Activin and Inhibin complexes which have wide-ranging effects on a  
348 variety of physiologic, homeostatic and metabolic processes including mammalian  
349 reproduction, inflammation and adipocyte differentiation (Woodruff and Mather 1995;  
350 Werner et al. 2006; Hirai et al. 2005). Interestingly, 13:0-24.24 Mb participates in five  
351 separate interactions that are significant in the full model (Table 1) and appears to interact  
352 with a region (9:68.10-95.10 Mb) containing an important receptor for serotonin (*Htr1b*).

353         Glutamate signaling and metabolism are also likely to underlie a portion of fatpad  
354 variation due to epistasis in this cross. The interacting epiQTL CI 1:42.41-52.71 Mb and  
355 9:68.10-95.10 Mb contain the enzyme that catalyses the first reaction in the primary  
356 pathway for the renal catabolism of glutamine (*Gls*) and the first rate limiting enzyme in  
357 glutathione synthesis (*Gclc*) respectively. *Gls* also shows differential expression in white  
358 fat cells between the parental lines ( $p = 0.00097$ ). Ghrelin and its associated pathways  
359 also appear as likely candidates. For example, 1:118.37-138.01 Mb contains *Gpr39*, a  
360 member of the ghrelin receptor family. This CI interacts with 6:133.92-142.67 Mb which  
361 harbors *Pde3a*, a locus known to be downstream of ghrelin signaling in platelets



362 (Elbatarny et al. 2007) and which shows significant differences in gene expression in  
363 white fat between SM/J and LG/J ( $p=0.00018$ ), and 12:73.42-89.12 Mb which contains  
364 *Hif1a*, whose protein product increases the expression of *Vegf* (Hoffmann et al. 2008).  
365 Interestingly, *Vegfc* shows a significant difference in expression in white fat between the  
366 parental lines ( $p = 0.001$ ) and *Vegfb* shows differences in liver ( $p = 0.009$ ). Ghrelin is  
367 also known to increase the expression of *Vegf* in human luteal cells (Tropea et al. 2007)  
368 and *Vegf* in turn, is thought to be an important regulator of adipogenesis and obesity (Cao  
369 2007). A final interesting epiQTL CI is 12:108.99-120.28 Mb. It contains *Dlk1*, *Meg3*,  
370 and *Rtl1*, all three of which appear to participate in an interacting (and imprinted)  
371 network affecting growth in mice (Gabory et al. 2009).

372

373

## DISCUSSION

374 While the family structure of an outbred population complicates some aspects of  
375 the mapping process, the  $F_{10}$  (and later) generations of advanced intercross lines hold an  
376 intrinsic advantage in mapping resolution over more conventional study designs. Here  
377 this advantage translated into a variety of results with important implications for mapping  
378 complex trait variation and new insights into the genetic architecture of murine fatpad  
379 weight.

380 The first and most striking result of this analysis from a mapping perspective is  
381 the relatively low level of overlap in the physical positions of sQTL and epiQTL peaks  
382 despite the analytical bias towards finding epistasis involving sQTLs due to their  
383 protected status with respect to multiple comparisons. Though slight discrepancies may  
384 be expected due to subtle patterns of linkage, larger map distances between peaks likely

385 indicate that multiple functional variants are present. Indeed, when both types are  
386 observed in close proximity, epistatic peaks tend not to line up well with their single-  
387 locus counterparts and epiQTL are frequently observed in regions showing no significant  
388 marginal effects at all (Figure 1; Table 1; Supplementary Table 1; Supplementary Figures  
389 1-20). This supports the notion that a relatively large number of variable, functionally  
390 relevant loci exert their influence on complex trait variation primarily via epistatic  
391 interactions rather than through conventional additive and dominance effects. It is also  
392 interesting to note that some regions interact with multiple locations in the genome. For  
393 example, proximal chromosome 13 (13:0-24.24 Mb) shows five significant interactions  
394 in the full model including two with separate locations on chromosome 1. Identifying  
395 such repeated signals may be useful in developing significance thresholds that help  
396 ameliorate the penalties incurred by performing multiple comparisons. Such consistency  
397 may also help distinguish epiQTL at the center versus the edges of functional networks.

398         Next, in keeping with observations in congenic lines (*e.g.* Christians et al. 2006)  
399 as well as other recent slQTL mapping studies (Fawcett et al. 2010),  $F_2$  confidence  
400 intervals were frequently observed to divide into multiple significant slQTL (Figure 1,  
401 Supplementary Figure 1). Interestingly, we observe similar splitting of single-locus and  
402 epistatic signals. For example, at the proximal end of chromosome 1 (Figure 1A)  
403 marginal effect peaks observed in the  $F_2$ , combined  $F_{2-3}$ , and in an intercross between SM  
404 and NZO (*obq7*; Taylor et al. 2001) appear to resolve in our mapping population into  
405 three distinct peaks with two marginal effect loci flanking an epiQTL. This suggests that  
406 the original  $F_2$  and the subsequent  $F_{2-3}$  signals in this cross were composites of both  
407 single-locus and epistatic effects and that the boundaries of previously reported CI may

408 have been influenced by epistatic contributions to single-locus values. Thus, current  
409 estimates of the number of loci underlying trait variation are likely to be overly  
410 conservative and reported effect size estimates are potentially biased by the presence of  
411 multiple, closely linked functional elements. Interestingly, it also suggests that  
412 confidence intervals identified in other intercross experiments, especially those that share  
413 a parental strain, can be productively evaluated under *a priori* epistatic hypotheses, which  
414 may also ease issues related to multiple testing. On this account, it is also striking that  
415 the epistatic network identified in Stylianou et al. (2006) as Chr4-*Adip11* is centered on a  
416 region also identified here as contributing to the epistatic architecture of fatpad weight.

417         The results of composite interval mapping also suggest that adjacent sQTL and  
418 epiQTL impact the mapping process. For example, there is a dramatic and unexpected  
419 increase in significance (nearly 3 orders of magnitude) for the additive sQTL peak at  
420 134.82 Mb on chromosome 1 when composite interval mapping was applied (Figure 1A).  
421 While this is the most dramatic example, such effects were repeatedly observed  
422 (Supplementary Figure 1) and on chromosomes 7 and 9 this resulted in the identification  
423 of two novel loci. Interestingly, this suggests that adjacent functional variants with  
424 opposite effects were fixed in the original parental lines during their production. Indeed,  
425 inspection of the regression coefficients from the full linear model shows that the  
426 epistatic peak closest to the sQTL signal at 134.82 Mb on chromosome 1 (DD with  
427 12:73.42-89.12 Mb) and the marginal signal itself share a positive sign. However, the  
428 two slightly centromeric interactions involving the additive value on chromosome 1 (AA  
429 with 13:0-24.24 Mb and AD with 6:133.92-142.67 Mb) are both negative. Conditioning  
430 on these adjacent markers is indeed expected to enhance the signal of the neighboring

431 additive effect, consistent with our observations. Thus, comparing the results of  
432 conventional single-locus mapping model and composite interval mapping may be an  
433 indirect means of identifying neighboring functional variants. Further mapping in later  
434 generations of this Advanced Intercross will provide a great deal of additional  
435 information on the sign, magnitude and physiological basis for these observed effects as  
436 recombination is expected to further separate their statistical signatures.

437         **Conclusions:** The application of multiple mapping approaches, including an  
438 epistatic model, is a vital strategy for characterizing complex genetic architectures.  
439 Contrary to suggestions based on human GWAS findings, we found substantial numbers  
440 of pair-wise epistatic interactions involving many more loci than show single locus  
441 effects that account for an important portion of trait variation. This is likely due to the  
442 genetic structure of our experimental population where allele frequencies are  
443 intermediate; there are no rare alleles in our mapping system. This is critical since  
444 epistasis is known to produce predominantly additive and dominance variance when  
445 relatively rare alleles are involved (Cheverud and Routman, 1995; Cheverud, 2000).

446         Here, the use of a combination of techniques was further enhanced by the  
447 improved genetic resolution offered by AI lines. While single locus scans remain the  
448 most tractable, pair-wise epistatic relationships can now be dissected in great detail as  
449 well and the identification of candidate loci for such interactions is possible. This is  
450 especially true for characters for which a large body of literature exists describing the  
451 mechanistic relationships among candidate genes and related pathologies. In such cases,  
452 incorporating *a priori* information regarding functional interactions can be used to help  
453 focus epistatic mapping studies and both ease the difficulties associated with multiple

454 comparisons and facilitate the physiological interpretation of statistical results. It is an  
455 exciting prospect that even more fine-scale mapping of these loci will be possible in later  
456 generations of the LG,SM AI line. Undoubtedly future analyses, coupled with the  
457 incorporation of sequence information from the parental lines, will aid in further refining  
458 the physiological hypotheses presented here for fatpad variation and greatly contribute to  
459 our understanding of the statistical signatures of complex genetic architectures.

460

461

#### ACKNOWLEDGEMENTS

462 The authors wish to acknowledge G. L. Fawcett and C. A. Lambert for offering  
463 insightful comments and suggestions on earlier drafts of this manuscript. This work was  
464 supported by a grant from the National Institutes of Health (DK-055736) and a Doctoral  
465 Dissertation Improvement Grant from the National Science Foundation (DEB-0608352).

466

466

LITERATURE CITED

- 467 Bartlett, M. S. and J. B. S. Haldane, 1935 The theory of inbreeding with forced  
468 heterozygosity. *J. Genet.* **31**: 327-340.
- 469 Bera, T. K., X-F Liu, M. Yamada, O. Gavrilova, E. Mezey, L. Tessarollo, M. Anver, Y.  
470 Hahn, B. Lee, and I. Pastan, 2008 A model for obesity and gigantism due to  
471 disruption of the *Ankrd26* gene. *PNAS.* **105(1)**: 270-257.
- 472 Brachya, G., C. Yanay and M. Linial, 2006 Synaptic proteins as multi-sensor devises of  
473 neurotransmission. *BMC Neuroscience.* **7(Suppl 1)**: S4.
- 474 Brockmann, G. A., C. S. Haley, U. Renne, S. A. Knott, and M. Schwerin, 1998  
475 Quantitative trait loci affecting body weight and fatness from a mouse line  
476 selected for extreme high growth. *Genetics.* **150**: 369-381.
- 477 Brockmann, G. A., J. Kratzsch, C. S. Haley, U. Renne, M. Schwerin, and S. Karle, 2000  
478 Single QTL effects, epistasis, and pleiotropy account for two-thirds of the  
479 phenotypic F(2) variance of growth and obesity in DU6i x DBA/2 mice. *Genome*  
480 *Res.* **10(12)**: 1941-1957.
- 481 Bult, C. J., J. T. Eppig, J. A. Kadin, J. E. Richardson, J.A. Blake and the members of the  
482 Mouse Genome Database Group, 2008 The Mouse Genome Database (MGD):  
483 mouse biology and model systems. *Nucleic Acids Res.* **36**: D724-728.
- 484 Cao, Y., 2007 Angiogenesis modulates adipogenesis and obesity. *J. Clin. Invest.* **117(9)**:  
485 2362-2368.
- 486 Chai, C., 1956a Analysis of quantitative inheritance of body size in mice I. Hybridization  
487 and maternal influence. *Genetics.* **41**: 157-164.

488 Chai, C., 1956b Analysis of quantitative inheritance of body size in mice. II. Gene action  
489 and segregation. *Genetics*. **41**: 165-178.

490 Chehab, F. F., 2008 Minireview: Obesity and lipodystrophy - Where do the circles  
491 intersect? *Endocrinology*. **149**: 925-934.

492 Cheverud, J. M., 2000 Detecting epistasis among quantitative trait loci. Pp. 58-81 *in* J. B.  
493 Wolf, E. D. Brodie, and M. J. Wade, eds. *Epistasis and the Evolutionary Process*.  
494 Oxford Univ. Press, Oxford.

495 Cheverud, J. M. and E. J. Routman, 1995 Epistasis and its contribution to genetic  
496 variance components. *Genetics* **139**:1455-1461.

497 Cheverud, J. M., G. L. Fawcett, J. P. Jarvis, E. A. Norgard, M. Pavlicev, L. S. Pletscher,  
498 K. S. Plonsky, H. Ye, G. I. Bell, and C. F. Semenkovich, 2010 Calpain-10 is a  
499 component of the obesity-related quantitative trait locus *Adip1*. *J. Lipid Res.* **51**:  
500 907-913.

501 Cheverud, J. M., T. H. Ehrich, J. P. Kenney, L. S. Pletscher, and C. F. Semenkovich,  
502 2004 Genetic evidence for discordance between obesity and diabetes-related  
503 traits in the LGXSM recombinant inbred mouse strains. *Diabetes*. **53**: 2700-2708.

504 Cheverud, J. M., T. H. Ehrich, T. Hrbek, J. P. Kenney, L. S. Pletscher, and C. F.  
505 Semenkovich, 2004 Quantitative trait loci for obesity and diabetes-related traits  
506 and their dietary responses to high fat feeding in the LGXSM recombinant inbred  
507 mouse strains. *Diabetes*. **53**: 3328-3336.

508 Cheverud, J. M., L. S. Pletscher, T. T. Vaughn, and B. Marshall, 1999 Differential  
509 response to dietary fat in large (LG/J) and small (SM/J) inbred mouse strains.  
510 *Physiol. Gen.* **1**: 33-39.

511 Cheverud, J. M., E. J. Routman, F. A. M. Duarte, B. van Swinderen, K. Cothran and C.  
512 Perel, 1996 Quantitative trait loci for murine growth. *Genetics*. **142**: 1305-1319.

513 Cheverud, J. M., T. T. Vaughn, L. S. Pletscher, A. C. Peripato, E. S. Adams, C. F.  
514 Erikson, K. J. King-Ellison, 2001 Genetic architecture of adiposity in the cross of  
515 LG/J and SM/J inbred mice. *Mam. Gen.* **12**: 3-12.

516 Christians, J. K., A. Hoeflich, and P. D. Keightley, 2006 *PAPPA2*, an enzyme that  
517 cleaves an insulin-like growth-factor-binding protein, is a candidate gene for a  
518 quantitative trait locus affecting body size in mice. *Genetics*. **173**: 1547-1553.

519 Corva, P. M., S. Horvat, and J. F. Medrano, 2001 Quantitative trait loci affecting growth  
520 in high growth (hg) mice. *Mamm Genome*. **12(4)**: 284-290.

521 Darvasi, A. and M. Soller, 1995 Advanced intercross lines, an experimental population  
522 for fine genetic mapping. *Genetics*. **141**: 1199-1207.

523 de Leeuw van Weenen, J. E., L. Hu, K. Jansen, Van Zelm, M. G. de Vries, J. T. Tamsma,  
524 J. A. Romijn, H. Pijl, 2009 Four weeks high fat feeding induces insulin resistance  
525 without affecting dopamine release or gene expression patterns in the  
526 hypothalamus of C57Bl6 mice. *Brain Res*. **1250**: 141-148.

527 Doria, A., M. Patti and C. Kahn, 2008 The emerging genetic architecture of type 2  
528 diabetes. *Cell Metabolism*. **8**: 186-200.

529 Duerr, R. H., K. D. Taylor, S. R. Brant, J. D. Rioux, M. S. Silverberg, M. J. Daly, A. H.  
530 Steinhart, C. Abraham, M. Regueiro, A. Griffiths, T. Dassopoulos, A. Bitton, H.  
531 Yang, S. Targan, L. W. Datta, E. O. Kistner, L. P. Schumm, A. T. Lee, P. K.  
532 Gregersen, M. M. Barmada, J. I. Rotter, D. L. Nicolae, J. H. Cho, 2006 A



533 Genome-Wide Association Study Identifies IL23R as an Inflammatory Bowel  
534 Disease Gene. *Science*. **314**: 1461-1463.

535 Elbatarny, H. S., S. J. Netherton, J. D. Ovens, A. V. Ferguson, and D. H. Maurice, 2007  
536 Adiponectin, ghrelin, and leptin differentially influence human platelet and  
537 human vascular endothelial cell functions: Implication in obesity-associated  
538 cardiovascular diseases. *Euro. J. Pharma*. **558**: 7-13.

539 Fawcett, G. L., C. C. Roseman, J. P. Jarvis, B. Wang, J. B. Wolf, and J. M. Cheverud,  
540 2008 Genetic architecture of adiposity and organ weight using combined  
541 generation QTL analysis. *Obesity*. **16**: 1861-1868.

542 Fawcett, G. L., J. P. Jarvis, C. C. Roseman, B. Wang, J. B. Wolf, and J. M. Cheverud  
543 2010 Fine-mapping of obesity-related quantitative trait loci in an F<sub>9/10</sub> advanced  
544 intercross line. *Obesity*. **18**(7):1383-1392.

545 Fenske, T. S., C. McMahon, D. Edwin, J. C. Jarvis, J. M. Cheverud, M. Minn, V.  
546 Mathews, M. A. Bogue, M. A. Province, H. L. McLeod, and T. A. Graubert, 2006  
547 Identification of Candidate Alkylator-Induced Cancer Susceptibility Genes by  
548 Whole Genome Scanning in Mice. *Cancer Res*. **66**: 5029-5038.

549 Gabory, A., M-A Ripoché, A. Le Digarcher, F. Watrin, A. Ziyat, T. Forne, H. Jammes,  
550 J. F. X. Ainscough, M. A. Surani, L. Journot, and L. Dandolo, 2009 *H19* acts as  
551 a trans regulator of the imprinted gene network controlling growth in mice.  
552 *Development*. **136**: 3413-3421.

553 Gardner, M., J. Bertranpetit, and D. Comas, 2008 Worldwide genetic variation in  
554 dopamine and serotonin pathway genes: Implications for association studies. *Am.*  
555 *J. Med. Genet. B*. **147B**(7): 1070-1075.

556 Gat-Yablonski, G. and M. Phillip, 2008 Leptin and regulation of linear growth. *Curr. Op.*  
557 *Clin. Nut. Met. Care.* **11**: 303-308.

558 Haldane, J. B. S. and C. H. Waddington, 1931 Inbreeding and Linkage. *Genetics.* **16**:  
559 357-374.

560 Haley, C. S. and S. A. Knott, 1992 A simple regression method for mapping quantitative  
561 trait loci in line crosses using flanking markers. *Heredity.* **69**: 315-324.

562 Hanlon P., W. A. Lorenz, Z. Shao, J. M. Harper, A. T. Galecki, R. A. Miller and D. T.  
563 Burke, 2006 Three-locus and four-locus QTL interactions influence mouse  
564 insulin-like growth factor-I. *Physiol. Genomics.* **26**:46-54.

565 Hanson, W. D., 1959a The theoretical distribution of lengths of parental gene blocks in  
566 the gametes of an F<sub>1</sub> individual. *Genetics.* **44**: 197-209.

567 Hanson, W. D., 1959b Theoretical distribution of the initial linkage block lengths intact  
568 in the gametes of a population intermated for n generations. *Genetics.* **44**: 839-  
569 846.

570 Hanson, W. D., 1959c Early generation analysis of lengths of heterozygous chromosome  
571 segments around a locus held heterozygous with backcrossing or selfing.  
572 *Genetics.* **44**: 833-837.

573 Hanson, W. D., 1959d The breakup of initial linkage blocks under selected mating  
574 systems. *Genetics.* **44**: 857-868.

575 Hirai, S., M. Yamanaka, H. Kawachi, T. Matsui, and H. Yano, 2005 Acitin A inhibits  
576 differentiation of 3T3-L1 preadipocyte. *Mol. and Cell. Endo.* **232**: 21-26.

577 Hoffmann, A-C, R. Mori, D. Vallbohmer, J. Brabender, E. Klein, U. Drebber, S. E.  
578 Baldus, J. Cooc, M. Azuma, R. Metzger, A. H. Hoelscher, K. D. Danenberg, K. L.

579           Prenzel, and P. V. Danenberg, 2008 High expression of *HIF1a* is a predictor of  
580           clinical outcome in patients with pancreatic ductal adenocarcinomas and  
581           correlated to *PDGFA*, *VEGF*, and *bFGF*. *Neoplasia*. **10(7)**: 674–679.

582   Horvat, S., L. Bunger, V. M. Falconer, P. Mackay, A. Law, G. Bulfield, and P. D.  
583           Keightley, 2000 Mapping of obesity QTLs in a cross between mouse lines  
584           divergently selected on fat content. *Mamm Genome*. **11(1)**: 2-7.

585   Ichihara, S. and Y. Yamada, 2008 Genetic factors for human obesity. *Cellular and*  
586           *Molecular Life Sciences*. **65**: 1086-1098.

587   Ishimori, N., R. Li, P. M. Kelmenson, R. Korstanje, K. A. Walsh, G. A. Churchill, K.  
588           Forsman-Semb, and B. Paigen, 2004 Quantitative trait loci that determine plasma  
589           lipids and obesity in C57BL/6J and 129S1/SvImJ inbred mice. *J Lipid Res*. **45(9)**:  
590           1624-1632.

591   Jannink, J.-L., M. C. A. M. Bink, and R. C. Jansen, 2001 Using complex plant pedigrees  
592           to map valuable genes. *Trends in Plant Science*. **6**: 337-342.

593   Jarvis, J. P., and J. M. Cheverud, 2009 Epistasis and the evolutionary dynamics of  
594           measured genotypic values during simulated serial bottlenecks. *J. Evol. Biol.* **22**:  
595           1658-1668.

596   Kahn, Z., S. Vijayakumar, T. Villanueva de la Torre, S. Rotolo, and A. Bafico, 2007  
597           Analysis of endogenous *LRP6* function reveals a novel feedback mechanism by  
598           which *Wnt* negatively regulates its receptor. *Mol. Cell. Biol.* **27**: 7291-7301.

599   Kamei, Y., H. Ohizumi, Y. Fujitani, T. Nemoto, T. Tanaka, N. Takahashi, T. Kawada, M.  
600           Miyoshi, O. Ezaki, A Kakizuka, 2003 PPAR $\gamma$  coactivator 1 $\beta$ /ERR ligand 1 is an

601 ERR protein ligand, whose expression induces a high-energy expenditure and  
602 antagonizes obesity. PNAS. **100**: 12378-12383.

603 Keightley, P. D., K. H. Morris, A. Ishikawa, V. M. Falconer, F. Oliver, 1998 Test of  
604 candidate gene--quantitative trait locus association applied to fatness in mice.  
605 Heredity. **81(Pt 6)**: 630-637.

606 Keightley, P. D., T. Hardge, L. May, and G. Bulfield, 1996 A genetic map of  
607 quantitative trait loci for body weight in the mouse. Genetics. **142**: 227-235.

608 Kenney-Hunt, J. P., B. Wang, E. A. Norgard, G. Fawcett, D. Falk, L. S. Pletscher, J. P.  
609 Jarvis, C. Roseman, J. Wolf, and J. M. Cheverud, 2008 Pleiotropic Patterns of  
610 Quantitative Trait Loci for 70 Murine Skeletal Traits. Genetics. **178**: 2275-2288.

611 Kim, J. H., S. Sen, C. S. Avery, E. Simpson, P. Chandler, P. M. Nishina, G. A. Churchill,  
612 and J. K. Naggert, 2001 Genetic analysis of a new mouse model for non-insulin-  
613 dependent diabetes. Genomics. **74(3)**: 273-286.

614 Klein, R. J., C. Zeiss, E. Y. Chew, J-Y Tsai, R. S. Sackler, C. Haynes, A. K. Henning, J.  
615 P. SanGiovanni, S. M. Mane, S. T. Mayne, M. B. Bracken, F. L. Ferris, J. Ott, C.  
616 Barnstable, J. Hoh, 2005 Complement Factor H Polymorphism in Age-Related  
617 Macular Degeneration. Science. **308**: 385-389.

618 Kramer, M. G., T. T. Vaughn, L. S. Pletscher, K. King-Ellison, E. Adams, C. Erikson,  
619 and James M. Cheverud, 1998 Genetic variation in body weight growth and  
620 composition in the intercross of Large (LG/J) and Small (SM/J) inbred strains of  
621 mice. Genet. Mol. Biol. **21**: 211-218.

622 Lander, E. S. and D. Botstein, 1989 Mapping mendelian factors underlying quantitative  
623 traits using RF.LP linkage maps [published erratum appears in Genetics 1994  
624 **136**: 705]. Genetics **121**: 185-199.

625 Lin, Y., X. Zhu, F. L. McIntee, H. Xiao, J. Zhang, M. Fu, and Y E. Chen, 2004  
626 Interferon Regulatory Factor-1 mediates PPAR $\gamma$ -Induced apoptosis in vascular  
627 smooth muscle cells. Arterioscler Thromb. Vasc. Biol. **24**: 257-263.

628 Mani, A., J. Radhakrishnan, H. Wang, A. Mani, M-A Mani, C. Nelson-Williams, K. S.  
629 Carew, S. Mane, H. Najmabadi, D. Wu, R. P Lifton, 2007 *LRP6* mutation in a  
630 family with early coronary disease and metabolic risk factors. Science.  
631 315(5816):1278-1282.

632 Maya-Monteiro, C. M., P. E. Almeida, H. D'Avila, A. S. Martins, A. P. Rezende, H.  
633 Castro-Faria-Neto, and P. T. Bozza, 2008 Leptin induces macrophage lipid body  
634 formation by a phosphatidylinositol 3-kinase and mammalian target of  
635 rapamycin-dependent mechanism. J. of Biol. Chem. **283**: 2203-2210.

636 Mehrabian, M., P. Z. Wen, J. Fisler, R. C. Davis, and A. J. Lusis, 1998 Genetic loci  
637 controlling body fat, lipoprotein metabolism, and insulin levels in a multifactorial  
638 mouse model. J Clin Invest. **101(11)**: 2485-2496.

639 Norgard, E. A., J. P. Jarvis, C. C. Roseman, T. J. Maxwell, J. P. Kenney-Hunt, K. E.  
640 Samocha, L. S. Pletscher, B. Wang, G. L. Fawcett, C. J. Leatherwood, J. B. Wolf  
641 and J. M. Cheverud, 2009 Replication of long bone length QTL in the F<sub>9</sub>-F<sub>10</sub>  
642 LG,SM Advanced Intercross. Mammalian Genome **20**: 224-235.

643 Papst, C., M. Bohn, H. F. Utz, A. E. Melchinger, D. Klein, J. Eder, 2004 QTL mapping  
644 for European corn borer resistance (*Ostrinia nubilalis* Hb.), agronomic and forage

645 quality traits of testcross progenies in early-maturing European maize (*Zea mays*  
646 L.) germplasm. *Theoretical and Applied Genetics* **108**: 1545-1554.

647 Phillips, P. C., 2008 Epistasis-the essential role of gene interactions in the structure and  
648 evolution of genetic systems. *Nat. Rev. Genet.* **9(11)**: 855-867.

649 R Development Core Team, 2009 R: A language and environment for statistical  
650 computing. R Foundation for Statistical Computing, Vienna, Austria. ISBN 3-  
651 900051-07-0, URL <http://www.R-project.org>.

652 Rockman, M. V. and L. Kruglyak, 2008 Breeding designs for recombinant inbred  
653 advanced intercross lines. *Genetics.* **179**: 1069-1078.

654 Rosen, C. J., C. Ackert-Bicknell, W. G. Beamer, T. Nelson, M. Adamo, P. Cohen, M. L.  
655 Boussein, and M. C. Horowitz, 2005 Allelic differences in a quantitative trait  
656 locus affecting insulin-like growth factor-I impact skeletal acquisition and body  
657 composition. *Pediatr Nephrol.* **20(3)**: 255-260.

658 Silver, L. M., 1995 *Mouse Genetics: Concepts and Applications*. Oxford University  
659 Press, New York.

660 Sladek, R., G. Rocheleau, J. Rung, C. Dina, L. Shen, D. Serre, P. Boutin, D. Vincent, A.  
661 Belisle, S. Hadjadj, B. Balkau, B. Heude, G. Charpentier, T. J. Hudson, A.  
662 Montpetit, A. V. Pshezhetsky, M. Prentki, B. I. Posner, D. J. Balding, D. Meyre,  
663 C. Polychronakos, and P. Froguel, 2007 A genome-wide association study  
664 identifies novel risk loci for type 2 diabetes. *Nature.* **445**: 881-885.

665 Smith Richards, B. K., B. N. Belton, A. C. Poole, J. J. Mancuso, G. A. Churchill, R. Li, J.  
666 Volaufova, A. Zuberi, and B. York, 2002 QTL analysis of self-selected

667 macronutrient diet intake: fat, carbohydrate, and total kilocalories. *Physiol*  
668 *Genomics*. **11(3)**: 205-217.

669 Sokal, R. S. and F. J. Rohlf, 1995 *Biometry*. W. H. Freeman and Company, New York.

670 Stylianou, I., M., R. Korstanje, R. Li, S. Sheehan, B. Paigen, G. A. Churchill, 2006  
671 Quantitative trait locus analysis for obesity reveals multiple networks of  
672 interacting loci. *Mammalian Genome* **17**: 22-36.

673 Taylor B. A., C. Wnek, D. Schroeder, and S. J. Phillips, 2001 Multiple obesity QTLs  
674 identified in an intercross between the NZO (New Zealand obese) and the SM  
675 (small) mouse strains. *Mamm Genome*. **12(2)**: 95-103.

676 Taylor, B. A., and S. J. Phillips, 1996 Detection of obesity QTLs on mouse  
677 chromosomes 1 and 7 by selective DNA pooling. *Genomics*. **34(3)**: 389-398.

678 Togawa, K., M. Moritani, H. Yaguchi, and M. Itakura, 2006 Multidimensional genome  
679 scans identify the combinations of genetic loci linked to diabetes-related  
680 phenotypes in mice. *Hum Mol Genet*. **15(1)**: 113-128.

681 Tontonoz, P., E. Hu, R. A. Graves, A. I. Budavari, and B. M. Spiegelman, 1994 mPPAR  
682 gamma 2: tissue-specific regulator of an adipocyte enhancer. *Genes and*  
683 *Development* **8**: 1224-1234.

684 Tropea, A., F. Tiberi, F. Minici, M. Orlando, M. F. Gangale, F. Romani, F. Miceli, S.  
685 Catino, S. Mancuso, M. Sanguinetti, A. Lansone, and R. Apa, 2007 Ghrelin  
686 affects the release of luteolytic and luteotropic factors in human luteal cells. *The*  
687 *Journal of Clinical Endocrinology & Metabolism* **92(8)**: 3239-3245.

688 Uchida, T., T. Nakamura, N. Hashimoto, T. Matsuda, K. Kotani, H. Sakaue, Y. Kido, Y.  
689 Hayashi, K. I. Nakayama, M. F. White, and M. Kasuga, 2005 Deletion of

690 Cdkn1b ameliorates hyperglycemia by maintaining compensatory  
691 hyperinsulinemia in diabetic mice. *Nature Medicine*. **11(2)**: 175-182.

692 Vaughn, T. T., L. S. Pletscher, A. Peripato, K. King-Ellison, E. Adams, C. Erikson, and J.  
693 M. Cheverud, 1999 Mapping quantitative trait loci for murine growth: a closer  
694 look at genetic architecture. *Genetical Research*. **74**: 313-22.

695 Warden, C. H., J. S. Fisler, S. M. Shoemaker, P. Z. Wen, K. L. Svenson, M. J. Pace, and  
696 A. J. Lusis, 1995 Identification of four chromosomal loci determining obesity in  
697 a multifactorial mouse model. *J Clin Invest*. **95(4)**: 1545-1552.

698 Watanabe, S., R. Yaginuma, K. Ikejima, and A. Miyazaki, 2008 Liver diseases and  
699 metabolic syndrome. *J. Gastroenterol*. **43**: 509-518.

700 Werner, S., C. Alzheimer, 2006 Roles of activin in tissue repair, fibrosis and  
701 inflammatory disease. *Cytokine & Growth Factor Reviews*. **17(3)**: 157-171.

702 Wentzell, A. M., H. C. Rowe, B. G. Hansen, C. Ticconi, B. A. Halkier, and D. J.  
703 Kliebensein, 2007 Linking Metabolic QTLs with Network and *cis*-eQTLs  
704 Controlling Biosynthetic Pathways. *PLoS Genetics* **3**: 1687-1701.

705 West, D. B., J. Goudey-Lefevre, B. York, G. E. Truett, 1994 Dietary obesity linked to  
706 genetic loci on chromosomes 9 and 15 in a polygenic mouse model. *J Clin Invest*.  
707 **94(4)**: 1410-1416.

708 Wilson, R. H., T. J. Morgan and T. F. C. Mackay, 2006 High-resolution mapping of  
709 quantitative trait loci affecting increased life span in *Drosophila melanogaster*.  
710 *Genetics*. **173**: 1455-1463.

711 Woodruff, T. K. and J. P. Mather, 1995 Inhibin, Activin and the female reproductive  
712 axis. *Annual Review of Physiology*. **57**: 219-244.



713 Yamauchi, T., Y. Nio, T. Maki, M. Kobayashi, T. Takazawa, M. Iwabu, M. Okada-  
714 Iwabu, S. Kawamoto, N. Kubota, T. Kubota, Y. Ito, J. Kamon, A. Tsuchida, K.  
715 Kumangai, H. Konzono, Y. Hada, H. Ogata, K. Tokuyama, M. Tsunoda, T. Ide,  
716 K. Murakami, M. Awazawa, I. Takamoto, P. Froguel, K. Hara, K. Tobe, R.  
717 Nagai, K. Ueki, and T. Kadowaki, 2007 Targeted disruption of *AdipoR1* and  
718 *AdipoR2* causes abrogation of adiponectin binding and metabolic actions. *Nature*  
719 *Medicine*. **13**: 332-339.

720 Yi, N., D. K. Zinniel, K. Kim, E. J. Eisen, A. Bartolucci, D. B. Allison, and D. Pomp,  
721 2006 Bayesian analyses of multiple epistatic QTL models for body weight and  
722 body composition in mice. *Genet Res*. **87(1)**: 45-60.

723 Yi, N., A. Diament, S. Chiu, K. Kim, D. B. Allison, J. S. Fisler, and C. H. Warden, 2004  
724 Characterization of epistasis influencing complex spontaneous obesity in the BSB  
725 model. *Genetics*. **167(1)**: 399-409.

726 Zeggini, E., L. J. Scott, R. Saxena, B. F. Voight, J. L. Marchini, T. Hu, P. I.W de Bakker,  
727 G. R. Abecasis, P. Almgren, G. Andersen, K. Ardlie, K. B. Boström, R. N.  
728 Bergman, L. L. Bonnycastle, K. Borch-Johnsen, N. P. Burtt, H. Chen, P. S.  
729 Chines, M. J. Daly, P. Deodhar, C. Ding, A. S. F. Doney, W. L. Duren, K. S.  
730 Elliott, M. R. Erdos, T. M. Frayling, R. M. Freathy, L. Gianniny, H. Grallert, N.  
731 Grarup, C. J. Groves, C. Guiducci, T. Hansen, C. Herder, G. A. Hitman, T. E.  
732 Hughes, B. Isomaa, A. U. Jackson, T. Jørgensen, A. Kong, K. Kubalanza, F. G.  
733 Kuruvilla, J. Kuusisto, C. Langenberg, H. Lango, T. Lauritzen, Y. Li, C. M.  
734 Lindgren, V. Lyssenko, A. F. Marvelle, C. Meisinger, K. Midthjell, K. L. Mohlke,  
735 M. A. Morken, A. D. Morris, N. Narisu, P. Nilsson, K. R. Owen, C. N. A. Palmer,

736 F. Payne, J. R. B. Perry, E. Pettersen, C. Platou, I. Prokopenko, L. Qi, L. Qin, N.  
737 W. Rayner, M. Rees, J. J. Roix, A. Sandbæk, B. Shields, M. Sjögren, V.  
738 Steinthorsdottir, H. M. Stringham, A. J. Swift, G. Thorleifsson, U.  
739 Thorsteinsdottir, N. J. Timpson, T. Tuomi, J. Tuomilehto, M. Walker, R. M.  
740 Watanabe, M. N. Weedon, C. J. Willer, Wellcome Trust Case Control  
741 Consortium, T. Illig, K. Hveem, F. B. Hu, M. Laakso, K. Stefansson, O. Pedersen,  
742 N. J. Wareham, I. Barroso, A. T. Hattersley, F. S. Collins, L. Groop, M. I.  
743 McCarthy, M. Boehnke, and D. Altshuler, 2008 Meta-analysis of genome-wide  
744 association data and large-scale replication identifies additional susceptibility loci  
745 for type 2 diabetes. *Nat Genet.* **40(5)**: 638–645.  
746 Zeng, Z. B., 1994 Precision mapping of quantitative trait loci. *Genetics.* **136**: 1457-68.  
747 Ziemke, F. and C. S. Mantzoros, 2010 Adiponectin in insulin resistance: lessons from  
748 translational research. *Am. J. Clin. Nutr.* **91(Suppl)**: 258S-261S.  
749

749 TABLE 1: Results from the full linear model of the epistatic network underlying murine  
750 reproductive fatpad weight in the LG,SM AI line. Chromosome, confidence intervals (Mb), peak  
751 locations (Mb), peak LPR scores, nearest SNP to the peak, effect type threshold and threshold  
752 value are all given for each term. The appropriate references for any *a priori* hypotheses are  
753 listed along with positional candidate loci for both sIQTL and epiQTL. Bold terms are nominally  
754 significant ( $p > 0.05$ ) when additive and dominance effects for all interactions are included in the  
755 model. References: <sup>1</sup>Cheverud et al. 2001; <sup>2</sup>Fawcett et al. 2008; <sup>3</sup>Taylor and Phillips 1996; <sup>4</sup>Taylor  
756 et al. 2001; <sup>5</sup>Cheverud et al. 2004; <sup>6</sup>Yi et al. 2006; <sup>7</sup>Ishimori et al. 2004; <sup>8</sup>Fawcett et al. 2010;  
757 <sup>9</sup>Stylianou et al. 2006; <sup>10</sup>Togawa et al. 2006; <sup>11</sup>Brockmann et al. 2000; <sup>12</sup>Warden et al. 1995;  
758 <sup>13</sup>Keightley et al. 1998; <sup>14</sup>Rosen et al. 2005; <sup>15</sup>Kim et al. 2001; <sup>16</sup>Yi et al. 2004; <sup>17</sup>Corva et al. 2001;  
759 <sup>18</sup>West et al. 1994; <sup>19</sup>Horvat et al. 2000; <sup>20</sup>Smith Richards et al. 2002; <sup>21</sup>Mehrabian et al. 1998.

760

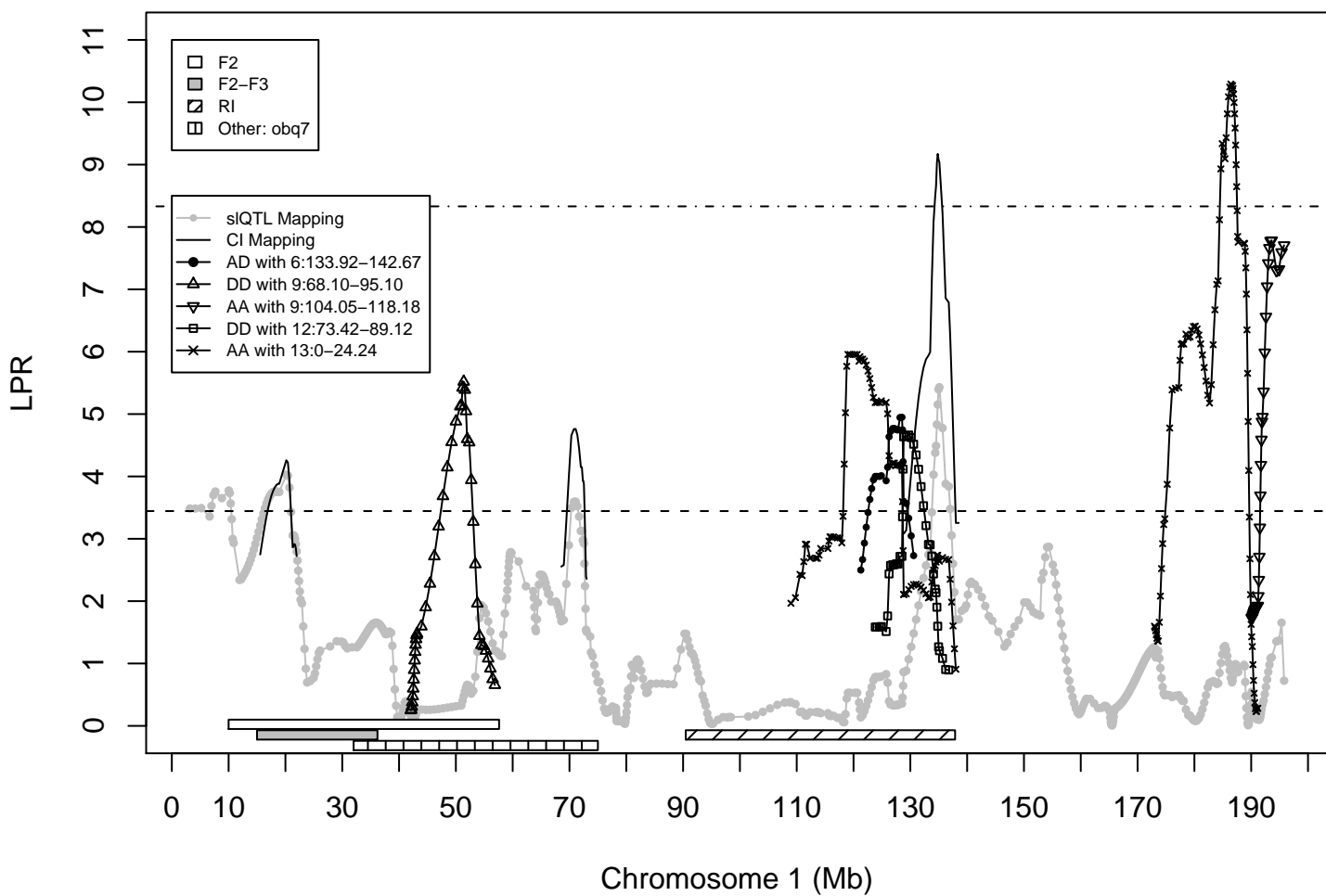
761

762 FIGURE 1: Mapping results of significant terms from the full model of reproductive fatpad weight  
763 in the LG,SM AI line for chromosomes 1 (A) and 13 (B). Results from the single-locus model are  
764 given as connected grey dots, composite interval mapping as smooth black lines and epistatic  
765 interactions by other connected shapes. Confidence intervals from previous analyses are  
766 represented by horizontal bars below the QTL plot.



Chr 1	CI 1 Begin (Mb)	CI 1 End (Mb)	Peak 1 (Mb)	Chr 2	CI 2 Begin (Mb)	CI 2 End (Mb)	Peak 2 (Mb)	sQTL LPR	Peak SNP 1	Peak SNP 2	Epistatic LPR	Effect(s)	Threshold Type	Threshold	Reported Adipose QTL in CI(s)	QTL Reference(s)	Candidates (CI 1)	Candidates (CI 2)
1	16.40	21.28	20.15	NA	NA	NA	NA	4.26	rs6334092	NA	NA	A,D	Pointwise	3.32	Adip1; Obq2	1:2;3	Pkh1	NA
1	65.79	74.08	70.77	NA	NA	NA	NA	4.76	rs6323094	NA	NA	A	Pointwise	6.60	Obq7	4	Vwz2; Fn1	NA
1	118.37	138.01	134.82	NA	NA	NA	NA	9.17	gnf01.132.831	NA	NA	A	Pointwise	3.32	Obst1; Gwth1; Obq17	5:6;7	Pk3c2b	NA
3	20.54	27.82	22.51	NA	NA	NA	NA	5.56	rs13477017	NA	NA	A	Pointwise	3.32	None	None	Nlgn1; Ghnr	NA
4	9.71	11.92	10.83	NA	NA	NA	NA	4.78	rs13477558	NA	NA	D	Pointwise	3.32	Unnamed RI QTL	5	Plekhl2	NA
4	78.28	90.30	79.46	NA	NA	NA	NA	11.87	CEL-4-78089985	NA	NA	A	Pointwise	3.32	Adip11; Adip24; Adip11a	2:8;9	Tyrp1	NA
6	114.73	121.97	117.73	NA	NA	NA	NA	5.01	mCV23042866	NA	NA	D	Pointwise	3.32	Adip2; Ig11s11	1:14	Adipor2; Ankd26; Ppang	NA
6	133.92	142.67	134.20	NA	NA	NA	NA	8.89	rs13479053	NA	NA	A	Pointwise	3.32	Adip2	1	Lrp6; Grn2b; Cdkn1b	NA
7	30.18	44.44	37.21	NA	NA	NA	NA	4.08	rs6217275	NA	NA	D	Pointwise	3.32	Adip3; Adip3A; Adip3Ab	1:2;8	Tshz3; Plekhf1	NA
7	59.83	77.73	63.51	NA	NA	NA	NA	6.85	rs3717293	NA	NA	A,D	Pointwise	3.32	Tabw; Adip3Ad; Adip25; Obq1	15:8;3	Nipa1; Nipa2; Gabrg3; Gabra5; Gabrb3	NA
7	132.03	143.20	135.24	NA	NA	NA	NA	6.38	CEL-7-116160192	NA	NA	A	New sQTL chr7	6.36	Bsbob2	16	Trim72	NA
8	64.98	90.95	84.79	NA	NA	NA	NA	4.76	rs13479860	NA	NA	A	Pointwise	3.32	Adip4	1:2	III5	NA
9	61.70	67.72	65.39	NA	NA	NA	NA	6.98	rs13480247	NA	NA	A	New sQTL chr9	6.38	None	None	Mfnt	NA
9	118.30	125.00	118.88	NA	NA	NA	NA	9.64	rs6316481	NA	NA	A	Pointwise	3.32	Adip5; Adip5a; Adip5b; Adip5c; Obq18	1:2;8;7	Acvr2b	NA
12	60.62	67.43	64.06	NA	NA	NA	NA	5.24	mCV24690992	NA	NA	A	Pointwise	3.32	Adip6; Adip16; Fob2	2:9;19	Lrnf5	NA
13	40.74	55.35	53.54	NA	NA	NA	NA	4.90	rs6999522	NA	NA	A	Pointwise	3.32	Adip7; Adip18; Adip18a; Pfat3	1:2;8;13	Cpl32; Hsd11a	NA
18	24.19	56.21	48.82	NA	NA	NA	NA	4.83	rs3684561	NA	NA	A	Pointwise	3.32	Adip8; Adip8a; Adip8b; Kcal1; Mnf2	1:8;20	Sema6a; Hsd11b4	NA
18	58.77	80.76	63.84	NA	NA	NA	NA	12.31	rs13483398	NA	NA	A	Pointwise	3.32	Adip8; Adip8a; Adip8b; Obsty4	1:2;8;5	Adrb2; Htr4	NA
1	42.41	52.71	51.38	9	68.10	95.10	77.25	NA	rs13475863	rs13480288	5.52	DD	QTL x QTL epi	3.44	Adip1; Obq7; Adip5; Mob8	1:4;21	Gis	Gclc
1	118.37	138.01	128.52	6	133.92	142.67	141.48	NA	rs6228473	rs8268650	4.95	AD	QTL x QTL epi	3.44	Obsty1; Gwth1; Obq17; Adip2	1:5;6;7	Gpr39	Pde3a
1	118.37	138.01	128.84	12	73.42	89.12	75.11	NA	rs13476100	rs3687032	4.64	DD	QTL x QTL epi	3.44	Obsty1; Gwth1; Obq17; Adip6	1:5;6;7	Gpr39	Hif1a
1	174.21	189.05	186.63	13	0.00	24.24	23.48	NA	mCV24555989	gnf13.020.621	10.27	AA	QTL x chr1 epi	5.25	Obq9	4	Hlx	Abt1
4	<b>30.53</b>	<b>39.16</b>	<b>36.58</b>	<b>9</b>	<b>118.30</b>	<b>125.00</b>	<b>123.70</b>	NA	<b>rs13477649</b>	<b>rs8241505</b>	<b>6.03</b>	<b>DD</b>	<b>QTL x QTL epi</b>	<b>3.44</b>	<b>Unnamed RI QTL; Dob2; Obq18</b>	<b>5:7;18</b>	<b>Cga</b>	<b>Slc6a20a; Slc6a20b</b>
4	125.68	139.92	130.91	7	132.03	143.20	139.70	NA	rs3673061	rs8236684	4.93	AD	QTL x QTL epi	3.44	Adip12; Qbs1; Afpq2; Adip3	1:9;10;11	Pprru	Oai
4	143.52	154.77	152.94	7	132.03	143.20	141.88	NA	rs6378384	rs3719258	4.69	AD	QTL x QTL epi	3.44	Adip12; Adip3	1:9	Ajpp1	Adam12
6	<b>33.46</b>	<b>46.84</b>	<b>37.64</b>	<b>9</b>	<b>118.30</b>	<b>125.00</b>	<b>123.70</b>	NA	<b>rs13478717</b>	<b>rs8241505</b>	<b>5.11</b>	<b>DA</b>	<b>QTL x chr6 epi</b>	<b>5.09</b>	<b>Dob2; Obq18</b>	<b>7:18</b>	<b>Trim24</b>	<b>Ccr9</b>
6	53.92	71.82	54.18	7	102.32	108.47	105.10	NA	rs13478762	UT-7-90.803899	5.13	AA	QTL x chr7 epi	4.96	Adip2; Obq13	1:4	Chrz2; Ghhr	Capn5
7	132.03	143.20	137.17	8	42.26	57.10	50.65	NA	rs8236684	rs13479769	5.08	AA	QTL x chr8 epi	4.73	Bsbob2	16	Egfr2	Ing2
8	124.83	129.12	127.97	9	20.24	39.76	23.57	NA	rs6500613	rs13480112	5.57	AD	QTL x chr9 epi	4.99	Obsty2	5	Disc1	Npsr1
9	20.24	39.76	31.31	12	108.99	120.28	111.04	NA	CEL-9-29909656	CEL-12-104545022	5.36	AA,DD	QTL x chr9 epi	4.99	Carf2g	17	Kcnj5	Dlk1; Meg3; Rtl1
9	104.05	118.18	109.62	1	191.98	NA	193.61	NA	rs3723953	rs13476308	7.78	AA	QTL x chr1 epi	5.99	Adip5; Dob2	1:18	Fbxw cluster	Nek2
12	108.99	120.28	113.11	1	191.98	NA	195.79	NA	rs13481651	rs13476312	6.06	DA	QTL x chr1 epi	5.25	Adip6; Bsbob4; Mob3	1:2;16;12	Traf3	Hsd11b1
13	0.00	24.24	14.85	1	118.37	138.01	119.02	NA	rs13481702	rs3694226	5.96	AA	QTL x chr1 epi	5.25	Adip7	1	Inhba	Inhb
13	0.00	24.24	17.38	9	68.10	95.10	82.84	NA	rs3678616	rs13480312	4.54	AA	QTL x QTL epi	3.44	Adip7; Adip5	1	Inhba	Htr1b
13	0.00	24.24	20.21	12	73.42	89.12	82.08	NA	rs6314295	rs3654718	4.78	AA	QTL x QTL epi	3.44	Adip7; Adip6	1	Inhba	Slc8a3
13	40.74	55.35	43.69	6	80.99	92.88	89.62	NA	rs13481789	rs13479099	4.90	AA	QTL x QTL epi	3.44	Adip7; Adip18; Adip18a; Pfat3; Adip2	1:2;8;13	Ranbp9	Alms1
13	40.74	55.35	45.45	4	143.52	154.77	152.94	NA	rs3688207	rs6378384	4.48	AD	QTL x QTL epi	3.44	Adip7; Adip18; Adip18a; Pfat3; Adip12	1:2;8;9;13	Atxn1	Kcnab2
18	24.19	56.21	37.51	12	60.62	67.43	64.06	NA	gnf18.033.953	mCV24690992	5.88	AD	QTL x QTL epi	3.44	Adip8; Adip8a; Adip8b; Kcal1; Mnf2; Adip6	1:8;20	Pcdhb cluster	Lrnf5
18	<b>24.19</b>	<b>56.21</b>	<b>37.93</b>	<b>13</b>	<b>0.00</b>	<b>24.24</b>	<b>15.11</b>	NA	<b>gnf18.033.953</b>	<b>rs13481702</b>	<b>5.87</b>	<b>DA</b>	<b>QTL x QTL epi</b>	<b>3.44</b>	<b>Adip8; Adip8a; Adip8b; Kcal1; Mnf2; Adip7</b>	<b>1:8;20</b>	<b>Pcdhb cluster</b>	<b>GH3</b>
18	24.19	56.21	50.47	7	30.18	44.44	30.56	NA	rs13483356	rs13479174	5.76	AD	QTL x QTL epi	3.44	Adip8; Adip8a; Adip8b; Kcal1; Mnf2; Adip3	1:8;20	Hsd11b4	Lrnf3

A)



B)

